Available online at www.eccomasproceedia.org
Eccomas Proceedia COMPDYN (2025) 977- 988

ECCOMAS
Proceedia

COMPDYN 2025
10th ECCOMAS Thematic Conference on
Computational Methods in Structural Dynamics and Earthquake Engineering
M. Papadrakakis, M. Fragiadakis (eds.)
Rhodes Island, Greece, 15-18 June 2025

ENVIRONMENTAL ANALYSIS–DRIVEN STRUCTURAL OPTIMIZATION FOR HYBRID STRUCTURAL SYSTEMS

Laura Sardone[1], Giulia Angelucci[2], Giuseppe Marano[1] and Fabrizio Mollaioli[2]

[1] Department of Structural, Geotechnical and Building Engineering
Polytechnic University of Turin
Corso Duca degli Abruzzi, 24, 10129 Torino, Italy
{laura.sardone, giuseppe.marano}@polito.it

[2] Department of Structural and Geotechnical Engineering
Sapienza University of Rome
via Gramsci, 53, 00197 Rome, Italy
{giulia.angelucci, fabrizio.mollaioli}@uniroma1.it

Abstract

Integrating Life Cycle Assessment (LCA) methodologies within Structural Design Optimization (SDO) is essential for advancing sustainable engineering practices. This study presents a robust framework that merges structural optimization techniques with LCA to assess and mitigate the environmental impacts associated with industrial steel-timber hybrid buildings.
Focusing on generative design applications, the research employs a Visual Programming Language (VPL) environment to optimize the size, shape, and topology of a single-story industrial space frame structure. The optimization process emphasizes material efficiency and Global Warming Potential (GWP) as key environmental metrics. Two primary scenarios are analyzed: one utilizing pure steel elements and the other permitting hybrid configurations that incorporate glulam timber. Multi-objective evolutionary algorithms (MOEAs) facilitate the identification of Pareto-optimal solutions, balancing structural performance with environmental considerations. Results indicate that hybrid configurations achieve substantial GWP reductions relative to conventional steel structures, while still delivering comparable structural integrity. Sensitivity analyses identify critical design variables—such as cross-sectional area, span lengths, and support conditions—that significantly affect the interplay between environmental and structural performance objectives. This research underscores the importance of incorporating environmental parameters early in the design process to foster sustainable practices within the construction sector.

Keywords: Life Cycle Assessment, Structural Optimization, Environmental Engineering, Steel Structures, Sustainable Construction.

ISSN:2623-3347
Peer-review under responsibility of the organizing committee of COMPDYN 2025.
doi: 10.7712/120125.12707.24971

1 INTRODUCTION

Structural Optimization (SO) integrates engineering principles and computational methodologies to achieve high-performance, lightweight designs [1]. Within the Architecture, Engineering, and Construction (AEC) sector, optimization techniques are applied to determine optimal design parameters for size (cross-sectional dimensions), shape (geometric boundaries), and topology (material distribution). By leveraging on advanced algorithms, SO effectively provides a powerful tool for navigating complex design spaces, balancing structural efficiency and material reduction [2-4].

Recent studies have confirmed the AEC industry as a major contributor to global carbon dioxide (CO_2) emissions and responsible for approximately 40% of worldwide greenhouse gas (GHG) emissions and energy consumption. The growing emphasis on environmental sustainability has compelled to reflect upon innovative approaches to building design, construction, and maintenance. To mitigate the AEC industry's environmental impact, advancements in SO offer promising strategies for enhancing resource efficiency and reducing environmental damage [5-7].

Life Cycle Assessment (LCA), as standardized by ISO 14044:2006 [8] and 14040:2006 [9], quantifies a product or system's environmental impact across its entire lifecycle, from raw material extraction to end-of-life disposal. In the SO context, LCA has been applied to various structural types to improve environmental performance. For instance, in building design, LCA-BIM integration facilitates comparative analysis of structural systems, enabling designers to prioritize actions that mitigate environmental burdens [10]. Advanced methodologies, such as Eco-OptiCAD, combine SO and LCA tools to enhance product environmental performance while maintaining structural and functional requirements [11]. With the ongoing evolution of this field, the development of sophisticated tools and methodologies that streamline the definition of sustainable structures is anticipated, strengthening the imperative to incorporate LCA within optimization frameworks (e.g., [12, 13]).

Despite significant efforts have been made to include LCA into SO for composite or reinforced concrete systems, research on steel and hybrid steel-timber structures remains comparatively limited. To address this, a Multi-Objective Optimization (MOO) framework is developed in this study to incorporate environmental and structural performance criteria for the optimal design of steel and hybrid space-frame structures. Employing a cradle-to-grave LCA approach, this framework provides comprehensive insights into the trade-offs between structural performance and environmental impact. Parametric design software using Visual Programming Language (VPL) and integrated derivative-free Multi-Objective Evolutionary Algorithms (MOEAs) support efficient exploration of complex design trade-offs, bridging the current gap in seamless LCA integration during early design phases.

2 OPTIMIZATION FRAMEWORK

The proposed methodology for the optimal design of space frame structures, is based on an integrated LCA and SO approach within a MOO framework. The framework aims to achieve a Pareto-optimal balance among structural performance, environmental impact, and practical feasibility. Size, shape, and topology optimization are performed concurrently, with LCA incorporated to assess material efficiency and environmental impact across the structure's lifecycle. Environmental impact is quantified in terms of Global Warming Potential (GWP) in kg CO_2 equivalents, adhering to European standards [14].

The main steps of the proposed procedure are illustrated in Figure 1.

Firstly, the parametric model is generated within a VPL environment, specifically Grasshopper (GH) for Rhinoceros via Python scripting.

Subsequently, finite element analysis (FEA), conducted using Karamba3D [17], initiates the optimization process. The built-in Karamba3D component enables structural simulation and verification in accordance with Eurocode 3 and 5 prescriptions [15, 16].

LCA is then incorporated, defining the product system, functional unit, system boundary, and data requirements. Material and process data are correlated with environmental data, and emission outputs are transformed into impact indicators during the Life Cycle Impact Assessment (LCIA) stage.

Upon retrieval of component-specific geometric, structural, and environmental data, the objective function (OF) is evaluated. A multi-objective strategy is preferred to simultaneously minimize structural mass and CO_2 emissions. The optimization problem is defined as a MOO problem, where the vector of design variables (**x**) is used to concurrently minimize two objective functions: OF_1 (structural mass) and OF_2 (environmental impact). These functions represent inherently conflicting design objectives. Reducing structural mass, which is desirable for material cost reduction, often requires higher-grade materials (e.g., high-strength steel). These materials typically have a greater environmental impact due to energy-intensive extraction, manufacturing, and transportation. Also lightweight, high-performance materials, such as advanced alloys or carbon fiber composites, could significantly reduce mass, but their embodied energy and manufacturing CO_2 emissions are substantially higher than conventional steel or timber. In this context, optimization procedures prove highly beneficial for the identification of compromise solutions.

Mathematically, the mass minimization function ($f_m(\mathbf{x})$) for a space-frame structure can be expressed by explicitly considering the individual contributions of beam-column elements and nodes, as follows:

$$\mathrm{OF}_1 = \min f_m(\mathbf{x}) = \min\left[\phi_1 \sum_{i=1}^{N} \rho_i A_i L_i + \phi_2 \sum_{j=1}^{M} M_{nod,j}\right] \tag{1}$$

where N and M are the total number of elements and node connections in the structural system, respectively; $M_{nod,j}$ is the mass of the j^{th} node; ρ_i, A_i and L_i are the material density, cross-section area, and length of the i^{th} element, respectively. This formulation accommodates heterogeneous material densities across the elements of the structural system, thereby enabling the optimization of hybrid solutions.

In Eq.(1), two penalty functions (ϕ_1 and ϕ_2) are enforced to penalize infeasible design solutions. Local performance checks ensure compliance with safety verifications prescribed in Eurocode 3 [15] for steel members or Eurocode 5 [16] for timber members, depending on the element's material. Non-compliant elements are penalized using the following function ϕ_1:

$$\phi_1 = 1 + n_k K_1 \tag{2}$$

where n_k is the number of structural members violating the performance constraints, and K_1=1.1 imposes a 10% penalty per failing member.

Function ϕ_2 penalizes solutions that lead to structural systems with an inconvenient high number of connections, as follows:

$$\phi_1 = 1 + n_k K_1 \tag{3}$$

where K_2 =1.1 applies a 10% penalty to all nodes within the structural system.

Consistent with the mass minimization function in Eq.(1), the GWP coefficients, representing CO_2 emissions, are expressed as the sum of contributions from beam and column elements ($GWP_{b/c}^{tot}$) and nodes (GWP_{nod}^{tot}), as follows:

$$\mathrm{OF}_2 = \min f_{GWP}(\mathbf{x}) = \min\left[\phi_1\phi_3 GWP_{b/c}^{tot} + \phi_2\sum_{j=1}^{M} M_{nod,j}\, GWP_{nod}^{tot}\right] \tag{4}$$

To enforce Serviceability Limit State (SLS) restrictions, an additional penalty function ϕ_3 is introduced:

$$\phi_3 = 1 + (\delta_{max} - \delta_k) \tag{5}$$

where δ_{max} is the maximum allowable deflection; δ_k is the actual deflection of the structural configuration at the current iteration. If deflections exceed δ_{max}, the penalty increases.

Finally, OF_1 and OF_2 are combined into a MOO formulation, which yields:

$$\mathrm{OF}_{1,2} = \min\left[\phi_1\phi_3\sum_{i=1}^{N}\rho_i A_i L_i\left(1 + GWP_{b/c}^{tot}\right) + \phi_2\sum_{j=1}^{M} M_{nod,j}\left(1 + GWP_{nod}^{tot}\right)\right] \tag{6}$$

Design variables encompass cross-section sizes (size optimization), nodal coordinates (shape optimization), and node connectivity (topology optimization). An initial parameter guess starts optimization. Optimization routines are performed within the GH-VPL environment, utilizing the Strength Pareto Evolutionary Algorithm II (SPEA-II) in Octopus [18]. This derivative-free Multi-Objective Evolutionary Algorithm-Graphical User Interface (MOEA-GUI) enables the exploration of multiple design configurations while ensuring compliance with technical code prescriptions. Design variables are iteratively adjusted to optimize the OF, with the algorithm refining the Pareto front beyond initial feasible solutions. Optimization terminates upon reaching the maximum iteration count or a 0.1% convergence threshold.

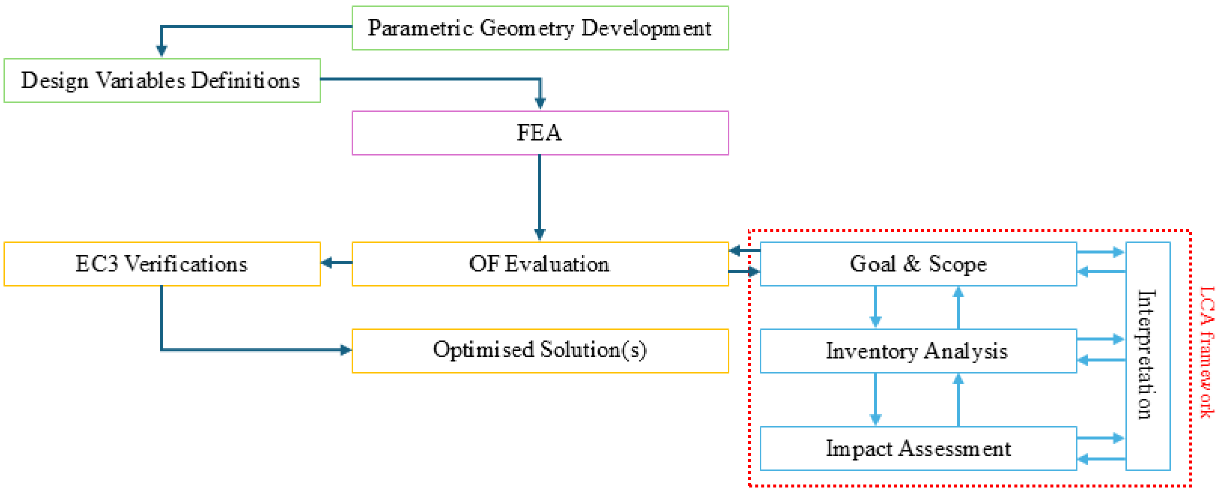

Figure 1: Flowchart of the optimization framework.

3 CASE STUDY

A simple case study is presented to demonstrate the practical applicability of the proposed optimization methodology in identifying efficient design solutions. The effective integration of LCA within the SO framework is applied to the design of a single-story frame structure.

Figure 2 illustrates the baseline geometry for optimization, targeting structural efficiency and minimized GWP. The roof system comprises a double-layered space-frame with dimensions of 60 meters in the x-direction (Lx) and 30 meters in the y-direction (Ly). Modularity and repetition are prioritized to ensure structural efficiency and cost-effectiveness. Diagonal members form a three-dimensional framework connecting the top and bottom chord planes. Vertical support is provided by 8 m columns, symmetrically positioned and fixed at the base.

A parametric digital model is generated in GH for Rhino3D via Python scripting, allowing real-time design variable updating during optimization. The optimization framework, operating within a fully parametric VPL environment, offers significant advantages. Its flexibility enables facile modification of input parameters (geometry, materials, loads), aiding rapid design space exploration and efficient evaluation of design alternatives. Moreover, it supports sensitivity analysis, providing insights into the impact of input parameters on structural performance and environmental impact. When integrated with optimization algorithms, the parametric model enables a computationally efficient search for global optima, minimizing the computational burden of complex system optimization.

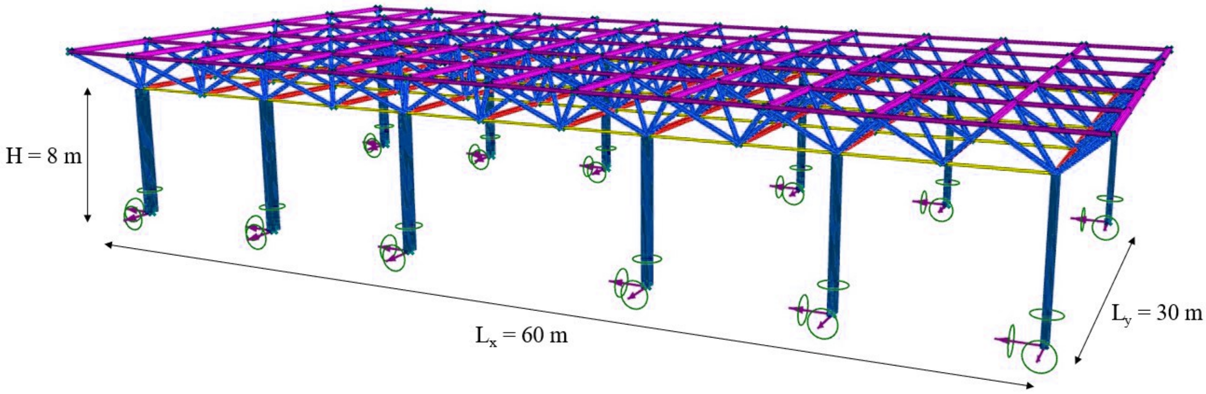

Figure 2: Three dimensional view of the reference structure.

Based on this geometry, the structural model, including elements, loads, and boundary conditions, is directly defined using Karamba3D - GH solver.

Prior to the initiation of the iterative optimization process, a clear definition of the design variables is established. These variables, which will be adjusted and optimized throughout the process, are categorized according to the distinct optimization domains of size, shape, and topology. This categorization ensures that all relevant aspects of the structural design are considered and optimized, allowing for a comprehensive exploration of the design space and the identification of optimal solutions.

The roof structure undergoes topological and shape optimization by adjusting its height (H) and the number of elements and nodes along the two horizontal directions (Lx and Ly). The roof truss overall height is initialized at 4 m, striking a balance material efficiency and structural rigidity. Joints are uniformly spaced to ensure even load distribution and minimize stress concentrations. The upper bound for H is set to a height-to-span ratio (H/L) of 1/15, where L is Lx in this case. A lower bound of 0.5 m for H is enforced to guarantee constructability and provide adequate structural depth to resist bending and deflection.

The frame span (Δ) is identified as a dependent parameter, its value directly determined by the number of subdivisions specified along the x and y axes (divx and divy), and the overall dimensions of the space-frame. The subdivisions are the independent design variables, and their values are constrained within predefined ranges. Minimum and maximum allowable spans (Δ) are indirectly controlled by the defined ranges of divx and divy, effectively limiting beam element lengths. In this study, the minimum and maximum span dimensions are set to 1 meter and 10 meters, respectively.

Alongside topology and shape optimization for the roof, size optimization is conducted for the entire structure, allowing for the simultaneous optimization of beam and column cross-sections (CSs). Two distinct scenarios are analyzed to highlight the impact of material selection: a pure steel configuration (Case Study 1) and a hybrid steel-glulam timber configuration (Case Study 2). This latter case specifically investigates the potential for integrating glulam-timber members with steel profiles to achieve a synergistic combination of structural efficiency and reduced environmental footprint.

This approach is motivated by the recognition that steel offers a high strength-to-weight ratio, while timber exhibits a significantly lower GWP compared to conventional construction materials, such as steel and concrete. The reduced GWP of timber is attributed to its inherent biogenic carbon sequestration and the lower energy intensity of its production processes. Consequently, the strategic utilization of timber is explored as a viable and effective strategy for pursuing sustainability objectives in structural design [19, 20].

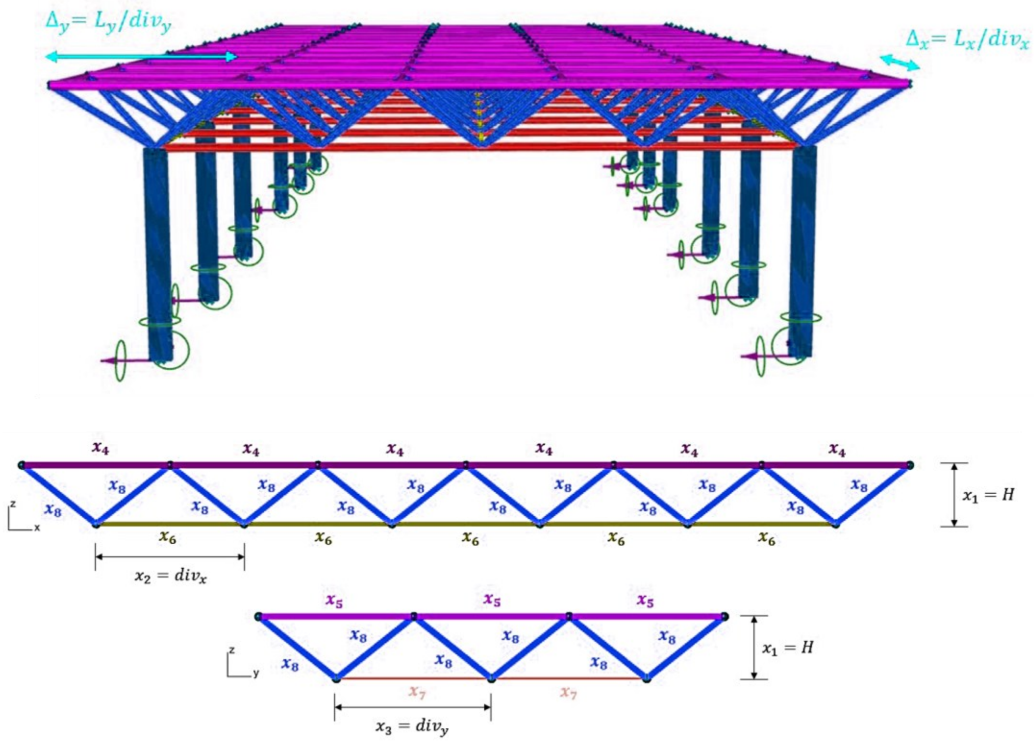

Figure 3: Three dimensional view (at the top) and longitudinal and transverse views (at the bottom) of the adopted clustering strategy for the roof elements with indication of the design variables.

To enhance material efficiency and reduce design variable dimensionality, frame elements are systematically categorizing into predefined groups (i.e., clusters) based on similar load distributions. Such strategy, which assigns identical CSs to elements experiencing comparable stress conditions, minimizes redundant evaluations and reduces the search space without compromising structural integrity. The main clusters comprise roof steel beams, roof diagonal members, and columns as vertical supports. Specifically, the design vector comprises:

a) upper and lower chords on x and y directions (4 design parameters) using steel Circular Hollow Section (CHS) or IPE profiles;
b) diagonals (1 design parameter) using steel CHS, steel double L-section or timber rectangular section;
c) columns (1 design parameter) using timber rectangular section.

The roof clustering strategy is depicted in Figure 3, wherein the five distinct clusters are identified by color. Roof elements can be assigned either open or closed CSs by the optimizer. As previously stated, the CSs designated for the diagonal elements enable the evaluation of two scenarios by the solver: steel sections or glulam sections.

Table 1 summarizes the design variables (x_i) and their respective upper and lower bounds (UL_{bounds}), defining the feasible design space. These bounds, derived from preliminary dimensioning and constructability considerations, ensure the optimization process yields structurally viable and manufacturable solutions.

The structural elements utilize steel S355 (Young's Modulus: 210 GPa) and glulam timber GL28h (Young's Modulus: 12 GPa) as material properties.

Applied loads include the self-weight of each component of the structure, automatically calculated by Karamba3D based on material properties and geometry. Additionally, permanent non-structural loads of 0.05 kN/m^2 and live loads of 0.5 kN/m^2 are applied to the roof system. A snow load of 1.23 kN/m^2 is incorporated, and wind loads are calculated according to the Eurocode (EN 1991-1-4), utilizing a base wind speed of 0.391 kN/m^2. Loads are combined according to the Ultimate Limit State (ULS) combination.

Description	x_i	UL_{bounds}
Roof Height	$x_1 = H$	[1, 3] (m)
Division on x-axis	$x_2 = div_x$	[6, 40] (integer)
Division on y-axis	$x_3 = div_y$	[3, 20] (integer)
Upper and lower chord CSs on x and y directions	$x_{[4,7]}$	[0, 170] IPE/CHS (solver index)
Diagonal CSs	x_8	[0 , 170] CHS/ 2L (solver index) [0, 201] CHS/2L/Glulam (solver index)
Column CSs	x_9	[0, 150] Glulam (solver index)

Table 1*:* Designeted design variables.

For each optimization iteration, a linear static FEA is executed in Karamba3D, and relevant performance parameters are recorded. These results are used to verify the load-bearing capacity, stability, and safety of the structural configurations in accordance with Eurocode 3-5 [15, 16]. Concurrently, the environmental impact is assessed by quantifying the GWP in kg CO_2 equivalent emissions, with LCA conducted in accordance with the EN 15804 for a comprehensive sustainability evaluation. This ensures a full cradle-to-grave assessment, providing accurate sustainability metric comparisons.

LCA data are integrated into the optimization process, quantifying Global Warming Potential (GWP) for key lifecycle stages: Production (A1-3), Installation/Assembly (A5), End-of-Life (C), and Recycling/Reuse potential (D). Production (A1-3) GWP values are: Closed steel profile = 1125 kgCO_2-eq./ton, Open steel profile = 3151.13 kgCO_2-eq./ton, Stainless steel screw = 4103 kgCO_2-eq./ton, and Glulam elements = -1294.468 kgCO_2-eq./ton. Installation/Assembly (A5) GWP, applicable only to steel profiles, is 0.817 kgCO_2-eq./m. End-of-Life (C) and Recycling/Reuse (D) GWP values are: Closed steel profile (C) = 0.621, (D) = -393 kgCO_2-eq./ton; Stainless steel screw (C) = 2.785, (D) = -1326 kgCO_2-eq./ton; and Glulam elements (C) = -1606.002, (D) = -872.127 kgCO_2-eq./ton. Steel recycling for primary steel reuse is neglected; glulam is assumed to undergo incineration with thermal energy recovery. The optimization process accounts for variations in material quantities during iterations.

4 RESULTS AND DISCUSSION

The penalty-based objective function $OF_{1,2}$ in Eq. (6) is evaluated by integrating LCA estimates and structural model data. Structural performance constraints, formulated according to Eurocode 3 for steel [15] and Eurocode 5 for timber [16], are implemented based on the CS type selected by the solver. To limit excessive deformation, serviceability constraints are applied. For steel elements, the maximum allowable deflection is set at L/300, while timber structures are constrained to L/300. In hybrid configurations, the more restrictive threshold is applied. The optimization process is driven by the Strength Pareto Evolutionary Algorithm II (SPEA-II), implemented within the Octopus plug-in.

Figure 4 presents the Pareto optimal fronts for the investigated case studies, depicting the trade-offs between structural mass and CO_2 emissions. To evaluate optimized designs, solutions S1, S2, and S3 are selected from these graphical representations. Selected solutions, representing extreme and intermediate designs, are compared against the Utopia Point (U). The optimization algorithm identifies the solution on the Pareto front that minimizes Euclidean distance to the U, thereby determining the best compromise.

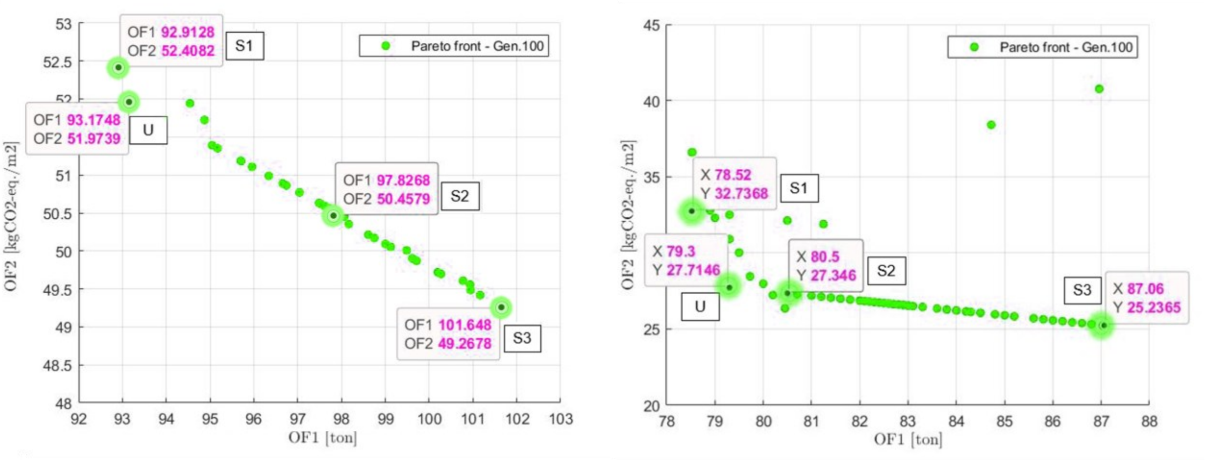

Figure 4: Pareto optimal fronts for Case Study 1 (on the left) and Case Study 2 (on the right).

Analysis of Case Study 1, which explores roof systems constructed exclusively from steel cross-sections, demonstrate a clear preference for closed steel sections within beam clusters. This selection is directly attributable to the enhanced torsional stiffness and overall structural capacity inherent in closed sections, a characteristic particularly advantageous in space-frame structures where torsional effects can be relevant.

Notably, a 6x3 modular configuration consistently emerge as optimal, effectively minimizing both component count and the structure's overall mass, in turn reducing embodied emissions. Furthermore, the roof height consistently converge towards its upper bound, stabilizing at 3 meters, a configuration that optimizes stress distribution throughout the space-frame. The constancy of connection counts and their associated GWP across all optimized solutions, as depicted in Figure 5, underscores the optimization process's focus on adjusting member sizes and material distribution, rather than altering the fundamental topology of the space-frame.

Expansion of the design space to incorporate timber diagonals yields a Pareto front (right-hand side of Figure 4) with a near-parabolic trend transitioning to a linear segment.

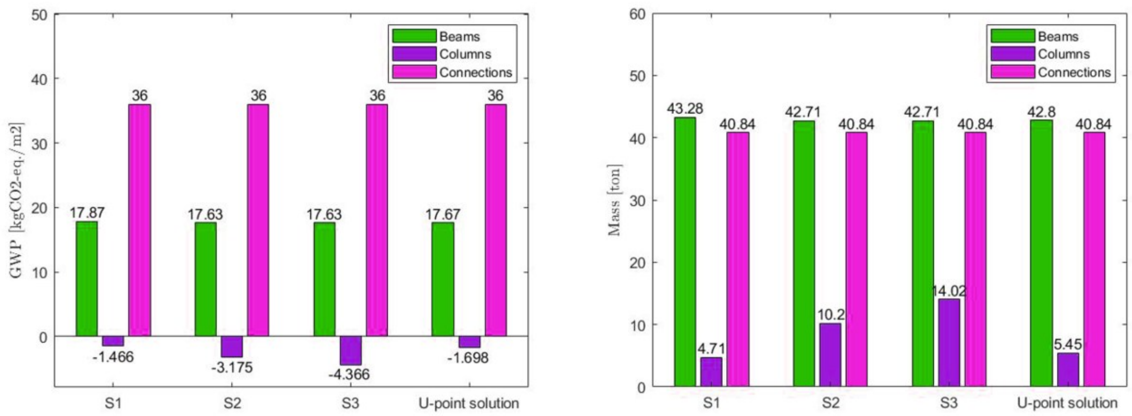

Figure 5: Case Study 1: GWP (on the left) and mass (on the right) contributions per structural member categories for optimal solutions.

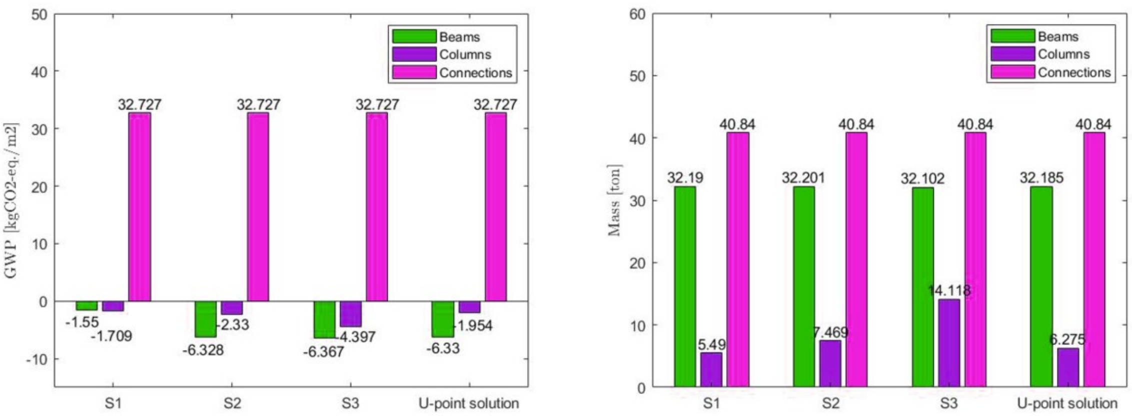

Figure 6: Case Study 2: GWP (on the left) and mass (on the right) contributions per structural member categories for optimal solutions.

Optimal designs regularly feature timber diagonals, exploiting timber's low density for lightweight solutions. Variations in diagonal and column cross-sections illustrate the optimizer's effort to balance mass and emission objectives.

Closed steel sections remained the preferred choice for chords, while rectangular glulam sections were favored for diagonals. This material selection achieved a 20% reduction in structural mass and a 45% reduction in GWP. The 6x3 modular layout maintained consistent connections and associated GWP. The production stage, particularly connection nodes (Figure 6), remained a significant carbon source. Beam component contributions varied with the selection of timber diagonals. Timber diagonals effectively reduced beam embodied energy. Despite larger column sections, the numerical dominance of diagonals (six times more than columns) resulted in a greater overall GWP reduction.

5 CONCLUSIONS

This study successfully demonstrates the efficacy of integrating Life Cycle Assessment (LCA) within a Structural Optimization (SO) framework for the sustainable design of hybrid framed structures. The parametric modeling approach, implemented in Grasshopper (GH), provides an accessible and efficient platform for preliminary design evaluations. Its Visual Programming Language (VPL) interface facilitates rapid exploration of design alternatives and seamless integration of structural analysis with LCA.

The framework's adaptability across diverse material types was validated through the optimization of a space-frame structure, adhering to Eurocode 3 and 5 prescriptions. The optimizer's ability to select hybrid material configurations, underscores its robustness and adaptability to varying material properties and design requirements. Multi-objective optimization (MOO), incorporating both structural and environmental objectives, revealed critical trade-offs and facilitated the identification of optimal compromise solutions. Notably, a 20% mass reduction and 45% Global Warming Potential (GWP) reduction were achieved, demonstrating the potential for significant sustainability improvements through integrated design strategies. The cradle-to-grave LCA, coupled with cross-sectional optimization and strategic material selection, proved effective in minimizing both material consumption and embodied energy. This research delivers a practical and adaptable framework for sustainable structural design. The integration of parametric modeling with LCA and MOO techniques empowers early-stage design decisions, enabling the development of resource-efficient and environmentally responsible structures. The methodology's alignment with global sustainable construction policies and its capacity to facilitate proactive compliance with carbon emission and resource efficiency regulations are significant.

ACKNOWLEDGMENTS

Dr. Laura Sardone carried out this study within the RETURN Extended Partnership and received funding from the European Union Next-GenerationEU (Piano Nazionale di Ripresa e Resilienza – PNRR, Mission 4, Component 2, Investment 1.3 – D.D. 1243 2/8/2022, PE0000005). Dr. Giulia Angelucci and Prof. Fabrizio Mollaioli gratefully acknowledge the financial support of PNRR (Piano Nazionale di Ripresa e Resilienza) – CN1 on "High-Performance Computing, Big Data and Quantum Computing" – Spoke 5 on "Environment and Natural Disaster: Framework and methodologies for impact evaluation and risk mitigation". Funding from the above research projects is greatly appreciated. The opinions and conclusions presented by the authors do not necessarily reflect those of the funding agencies.

REFERENCES

[1] M. Bremicker, P.Y. Papalambros, M. Chirehdast, N. Kikuchi, Integrated Topology and Shape Optimization in Structural Design. *Mechanics of Structures and Machines*, **19**(4), 551–587, 1991. https://doi.org/10.1080/08905459108905156

[2] G. Angelucci, S.M. Spence, F. Mollaioli, An integrated topology optimization framework for three-dimensional domains using shell elements. *The Structural Design of Tall and Special Buildings*, **30**(1), e1817, 2021. http://dx.doi.org/10.1002/tal.1817

[3] G. Angelucci, G. Quaranta, F. Mollaioli, Topology optimization of multi-story buildings under fully non-stationary stochastic seismic ground motion. *Structural and Multidisciplinary Optimization*, **65**(8), 217, 2022. http://dx.doi.org/10.1007/s00158-022-03319-5

[4] X. Meng, Y. Xiong, Y.M. Xie, Y. Sun, Z.L. Zhao, Shape–thickness–topology coupled optimization of free-form shells. *Automation in Construction*, **142**, 104476, 2022. https://doi.org/10.1016/j.autcon.2022.104476

[5] D. Yeo, R.D. Gabbai, Sustainable design of reinforced concrete structures through embodied energy optimization. *Energy and buildings*, **43**(8), 2028-2033, 2011. http://dx.doi.org/10.1016/j.enbuild.2011.04.014

[6] E. Frangedaki, L. Sardone, N.D. Lagaros, Design Optimization of Tree-Shaped Structural Systems and Sustainable Architecture Using Bamboo and Earthen Materials. *Journal of Architectural Engineering*, **27**(4), 2021. https://doi.org/10.1061/(ASCE)AE.1943-5568.0000492

[7] L. Sardone, A. Fiore, A. Manuello, R. Greco, Performative Structural Design Optimization: Generative Algorithm for a Preliminary Study of a Voided Beam. *Applied Sciences*, **12**(17), 8663, 2022. https://doi.org/10.3390/app12178663

[8] ISO 14044:2006. *Environmental management - Life cycle assessment – Requirements and guidelines*. International Organization for Standardization, Geneva, 2006.

[9] ISO 14040:2006. *Environmental management — Life cycle assessment — Principles and framework*. International Organization for Standardization, London, 2006.

[10] D.M.A. Morsi, A.A.E. Othman, A. Ehab, W.S.E. Ismaeel, BIM-based life cycle assessment for different structural system scenarios of a residential building. *Ain Shams Engineering Journal*, **13**(6), 101802, 2022. https://doi.org/10.1016/j.asej.2022.101802

[11] D. Russo, M. Serafini, Anticipating the Identification of Contradictions in Eco-design Problems. *Procedia Engineering*, **131**, 1011-1020, 2015. https://doi.org/10.1016/j.proeng.2015.12.419

[12] L. Jacquemin, P.Y. Pontalier, C. Sablayrolles, Life cycle assessment (LCA) applied to the process industry: a review. *The International Journal of Life Cycle Assessment*, **17**(8):1028–1041, 2012. https://doi.org/10.1007/s11367-012-0432-9

[13] J. Tao, Z. Chen, S. Yu, Z. Liu, Integration of Life Cycle Assessment with computer-aided product development by a feature-based approach. *Journal of Cleaner Production*, **143**, 1144–1164, 2016. https://doi.org/10.1016/j.jclepro.2016.12.005

[14] EN 15804:2012+A2:2019. *Sustainability of construction works - Environmental product declarations - Core rules for the product category of construction products*. The British Standards Institution, 2022.

[15] EN 1993-1-1, *Eurocode 3: Design of steel structures - Part 1-1: General rules and rules for buildings*, European Committee for Standardization, 2011.

[16] EN 1995-1-1, *Eurocode 5: Design of timber structures - Part 1-1: General - Common rules and rules for buildings*. European Committee for Standardization, 2008.

[17] C. Preisinger, M. Heimrath, Karamba—A Toolkit for Parametric Structural Design. *Structural Engineering International*, **24**(2), 217–221, 2014. https://doi.org/10.2749/101686614x13830790993483

[18] E. Zitzler, M. Laumanns, L. Thiele, SPEA2: Improving the strength pareto evolutionary algorithm. *TIK report*, **103**, 2001. https://doi.org/10.3929/ethz-a-004284029

[19] R. Laguardia, P. Franchin, S. Tesfamariam, Risk-based optimization of concentrically braced tall timber buildings: Derivative free optimization algorithm. *Earthquake Engineering & Structural Dynamics*, **53**(1), 179-199, 2024. http://dx.doi.org/10.1002/eqe.4015

[20] G. Angelucci, F. Mollaioli, M. Molle, S. Paris, Performance assessment of timber high-rise buildings: Structural and technological considerations. *The Open Construction & Building Technology Journal*, **16**(1), 1-12, 2022. http://dx.doi.org/10.2174/18748368-v16-e2206270